

# Technical Notes

*TECHNICAL NOTES are short manuscripts describing new developments or important results of a preliminary nature. These Notes cannot exceed 6 manuscript pages and 3 figures; a page of text may be substituted for a figure and vice versa. After informal review by the editors, they may be published within a few months of the date of receipt. Style requirements are the same as for regular contributions (see inside back cover).*

## Spanwise Averaging of Plane Mixing Layer Properties

James H. Bell\*

NASA Ames Research Center,  
Moffett Field, California 94035

and

Michael W. Plesniak† and Rabindra D. Mehta‡  
Stanford University, Stanford, California 94305

### Introduction

THE conventional view of a plane mixing layer has been that its structure is dominated by the presence of large organized spanwise vortices.<sup>1</sup> The spanwise vortices are generated through the Kelvin-Helmholtz instability, and the mixing layer then grows through entrainment by these vortices and their subsequent pairings. Recent flow visualization studies have shown that, for mixing layers originating from laminar initial boundary layers, there is the additional presence of organized streamwise vorticity that is spatially stationary and rides among the spanwise vortices.<sup>2</sup> These streamwise structures first appear in the braids (between the spanwise structures) before propagating into the spanwise vortex cores.

Bell and Mehta<sup>3</sup> recently studied (quantitatively) the origin and evolution of the streamwise vorticity in a plane mixing layer. Measurements of the mean streamwise vorticity indicated that small disturbances present in the incoming flow were initially amplified just downstream of the first spanwise roll-up, leading to the formation of concentrated streamwise vortices. The streamwise vortices first appeared in clusters containing vorticity of both signs, but farther downstream, the vortices reorganized to form a row of counter-rotating vortices. The streamwise vortex structure was found to grow in size, scaling approximately with the mixing layer vorticity thickness. The structure also weakened with downstream distance, the maximum mean vorticity decaying as approximately  $X^{-1.5}$ .

In the near field, the streamwise vortex structure was found to have a significant effect on the mixing layer mean and turbulence properties. The mean velocity and Reynolds stress contours exhibited large spanwise variations that became spatially quasiperiodic once a regular array of streamwise vortices was established. Large spanwise variations in the mixing layer

thickness and peak Reynolds stress levels were also observed in the near field of the mixing layer. Therefore, to adequately study the streamwise evolution of the mixing layer, it was felt that the layer properties ought to be spanwise averaged. This may be particularly critical when comparing the development of mixing layers with varying initial and operating conditions.<sup>4</sup>

The main objective of this Note is to demonstrate the effects of the streamwise vorticity on some of the mixing layer global properties, such as the layer thickness and peak Reynolds stresses. In particular, the interest is in the differences between results obtained from spanwise averaging over a number of velocity profiles and those given by the more conventional approach of just analyzing a single profile measured along the test section centerline.

### Experimental Apparatus and Techniques

The experiments were conducted in a mixing layer wind tunnel,<sup>3</sup> the main feature of which is its two separately driven legs that allow freestream velocities to be varied independently. In the present experiments, the two sides of the wind tunnel were run at freestream velocities of 9 and 15 m/s, thus giving a mixing layer with velocity ratio  $U_2/U_1 = 0.6$ . Throughout the present study,  $X$  is defined as the streamwise direction,  $Y$  the direction normal to the mixing layer, and  $Z$  the spanwise direction. The test section sidewalls were adjusted to give an approximately zero streamwise pressure gradient. The initial boundary layers were laminar and nominally two dimensional; some of their measured properties are summarized in Table 1.

Measurements were made using a rotatable cross-wire probe held on a three-dimensional traverse and linked to a fully automated data acquisition and reduction system controlled by a MicroVax II computer. The cross-wire probe had 5- $\mu$ m-diam tungsten sensing elements about 1 mm long and positioned about 1 mm apart. The probe was calibrated statically in the potential core of the flow assuming a cosine-law response to yaw, with the effective angle determined by calibration. The analog signals were low-pass filtered, dc offset, and amplified before being fed into a computer interface. The interface contained a fast sample-and-hold A/D converter with 12-bit resolution and a multiplexer for connection to the computer.<sup>3</sup> Individual statistics were averaged over 5000 samples obtained at a rate of 400 samples/s.

Data were obtained on large cross-plane grids at nine streamwise locations. Typically, at a given station, measurements were obtained at 1000–2000 spatial locations on a rectangular cross-plane grid. The measurements were corrected for mean streamwise velocity gradient effects and flow temperature variations.<sup>3</sup> The measurement accuracies are presented here in terms of the repeatability of the individual quantities. Measurements of  $U$  were repeatable to within 3% and those of the primary shear stress ( $u'v'$ ) to within 15%.

The spanwise averaged quantities were evaluated by dividing the measurements obtained on the cross-plane grid into individual  $Y$ -wise profiles or "slices" through the mixing layer. The mixing layer properties for each slice were computed in the traditional manner and then averaged with those obtained at all of the other spanwise positions, giving a single value for each quantity. In effect, the properties were aver-

Received Dec. 17, 1990; revision received April 15, 1991; accepted for publication April 23, 1991. Copyright © 1991 by the American Institute of Aeronautics and Astronautics, Inc. All rights reserved. No copyright is asserted under Title 17, U.S. Code. The U.S. Government has a royalty-free license to exercise all rights under the copyright claimed herein for Governmental purposes. All other rights are reserved by the copyright owner.

\*Research Scientist, Fluid Dynamics Research Branch, Mail Stop 260-1, Member AIAA.

†Postdoctoral Fellow, Department of Mechanical Engineering, Thermosciences Division; currently at School of Mechanical Engineering, Purdue University, West Lafayette, IN. Member AIAA.

‡Senior Research Associate, Department of Aeronautics and Astronautics, Joint Inst. for Aeronautics and Astronautics.

aged over 20–90 individual spanwise profiles covering a spanwise extent equivalent to 5–50 mixing layer thicknesses.

### Results and Discussion

To illustrate the implications of conclusions based only on centerline data, the same data were processed in two ways: 1) results were averaged across the span, as described earlier, and 2) only the centerline profile was considered, as typically done in the past.

Figure 1 shows the streamwise development of the mixing layer thickness  $\delta$  determined by the two methods. In both cases,  $\delta$  is evaluated from a two parameter optimization fit of the mean streamwise velocity profile to an error function. Growth rates based on a linear least-squares fit to  $\delta$  downstream of  $X=77$  cm were computed, yielding values of 0.023 and 0.021 for the spanwise averaged and centerline-based data, respectively. The difference in growth rate given by the two methods is about 9%. This difference cannot be solely attributed to measurement uncertainty, which for this quantity is estimated at around 5%. In addition, the spanwise averaged results seem to exhibit a better linear correlation; the error in the least-squares fit (goodness of fit parameter) is 0.025 for the averaged data and 0.060 for the centerline data. This is partly due to the fact that the data point at  $X=77.6$  cm fits on the same line as the downstream points in the averaged case, whereas the corresponding point in the centerline data is well below a straight line determined by fitting the last four points. Considering only the centerline data might lead one to conclude that the linear growth region is attained downstream of  $X=100$  cm, whereas the averaged data implies that linear growth is achieved farther upstream. It is worth noting that small relative differences in the mixing layer thickness in the downstream region can translate into significant differences in the evaluated growth rate.

The most dramatically affected quantity was the Reynolds primary shear stress  $u'v'$ , the streamwise evolution of which is illustrated in Fig. 2. The maximum shear stress is normalized by the velocity difference across the mixing layer ( $U_0 = U_1 - U_2$ ). The error bars on the spanwise averaged data indicate a  $\pm 1$  standard deviation of  $u'v'_{\max}$  across the span.

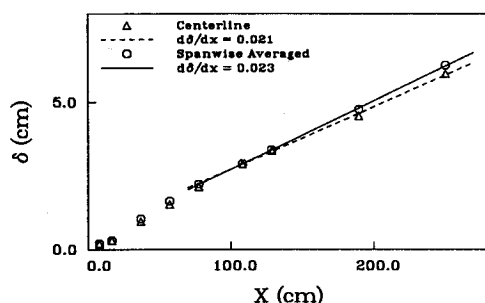


Fig. 1 Comparison of the streamwise development of the spanwise averaged and centerline value of the mixing layer thickness.

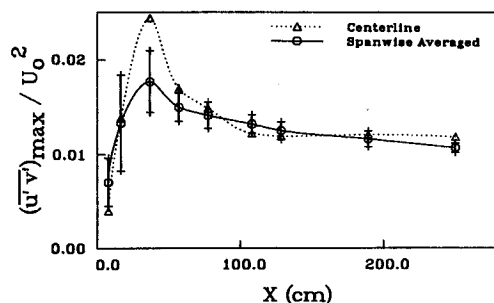


Fig. 2 Comparison of the streamwise development of the spanwise averaged and centerline value of the maximum primary Reynolds shear stress. Error bars indicate  $\pm 1$  standard deviation of  $u'v'_{\max}$  across the span.

Table 1 Initial boundary-layer properties

Condition	$U_e$ , m/s	$\delta_{99}$ , cm	$\theta$ , cm	$Re_\theta$	$H$
High-speed side	15.0	0.40	0.050	525	2.52
Low-speed side	9.0	0.44	0.061	362	2.24

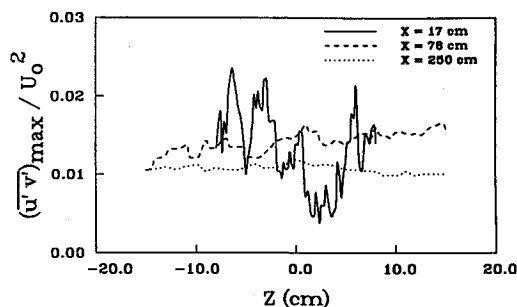


Fig. 3 Spanwise variation of the maximum primary Reynolds shear stress at three representative streamwise locations.

Note that the error bars are not an indication of measurement uncertainty, but are used to emphasize the relatively large spanwise variations and differences between the levels given by the two techniques, especially in the near field. The nature of the spanwise variation is shown in more detail in Fig. 3, in which the distribution of  $u'v'_{\max}$  with  $Z$  is plotted for three representative stations. Large spanwise variations of up to 40% are seen in the near-field region, but due to the decay of the streamwise vorticity, the variations drop to around 5% by the last measurement station.

As a consequence, the differences between the spanwise averaged levels and those given by the centerline profile in Fig. 2 are relatively large in the near-field region—the apparent agreement at  $X=17$  cm is totally fortuitous, as indicated by the results in Fig. 3. In particular, the centerline value at  $X=37$  cm is 40% higher than the spanwise averaged value. Only in the far downstream region, where the layer is quasi-two-dimensional are centerline results representative of the averaged mixing layer characteristics. Note that the centerline data seem to have approached an asymptotic level beyond  $X \sim 100$  cm, whereas the spanwise averaged data exhibit a slow monotonic decrease with streamwise distance. In comparing the two data sets, one may erroneously conclude that the mixing layer has achieved self-similarity due to the (perhaps fortuitous) constant level of Reynolds shear stress exhibited by the centerline data. The spanwise averaged data indicate that the mixing layer structure is still changing, albeit very slowly, right up to the end of the measurement domain. A very careful examination of all of the Reynolds stresses indeed shows that the present mixing layer does not satisfy all of the requirements for self-similarity until toward the end of the measurement domain.<sup>4</sup>

The streamwise evolution of the Reynolds normal stresses ( $u'^2$ ,  $v'^2$ , and  $w'^2$ ) is not presented here since it was qualitatively similar to that of  $u'v'$ . Relatively large differences between the spanwise averaged and centerline data were noted in the near field ( $X \leq 100$  cm), although the normal stress maxima asymptoted to comparable levels in the far field.

### Conclusions

Relatively large spanwise variations have been documented in the mean flow and turbulence properties of mixing layers developing from laminar initial boundary layers. These variations are caused by the presence of spatially stationary streamwise vortices that ride among the spanwise vortical structures. It is shown, by comparing the centerline and spanwise averaged results taken from the same data set, that significant misinter-

pretations regarding the development of the mixing layer may be drawn based solely on centerline data. In particular, the growth rate and streamwise development of peak Reynolds stresses in the near field can be affected significantly by spanwise variations in the mixing layer. It is proposed here that some of the discrepancies in the past regarding growth rates and approach to self-similarity may have been caused by the lack of spanwise averaging. It is particularly important to employ spanwise averaging when comparing the development of mixing layers with different initial and operating conditions.

### Acknowledgments

This research was supported by NASA Grant NCC-2-55 from the Fluid Dynamics Research Branch, NASA Ames Research Center, and a National Science Foundation Grant NSF-MSM-88-15670.

### References

- <sup>1</sup>Brown, G. L., and Roshko, A., "On Density Effects and Large Structure in Turbulent Mixing Layers," *Journal of Fluid Mechanics*, Vol. 64, Pt. 4, 1974, pp. 775-816.
- <sup>2</sup>Lasheras, J. C., Cho., J. S., and Maxworthy, T., "On the Origin and Evolution of Streamwise Vortical Structures in a Plane, Free Shear Layer," *Journal of Fluid Mechanics*, Vol. 172, 1986, pp. 231-258.
- <sup>3</sup>Bell, J. H., and Mehta, R. D., "Three-Dimensional Structure of Plane Mixing Layers," Dept. of Aeronautics and Astronautics, Stanford Univ., Stanford, CA, JIAA TR-90, March 1989.
- <sup>4</sup>Bell, J. H., and Mehta, R. D., "Development of a Two-Stream Mixing Layer From Tripped and Untripped Boundary Layers," *AIAA Journal*, Vol. 28, No. 12, 1990, pp. 2034-2042.

## Approximate Formula of Weak Oblique Shock Wave Angle

Hua-Shu Dou\* and Hsueh-Ying Teng†  
Beijing University of Aeronautics and Astronautics,  
Beijing, People's Republic of China

### Introduction

IN the theory of oblique shock waves, the deflection angle  $\theta$  of flow across an oblique shock is related to the wave angle  $\beta$  by Eq. (1)<sup>1-3</sup>:

$$\frac{\tan(\beta - \theta)}{\tan\beta} = \frac{(\gamma - 1)M_1^2 \sin^2\beta + 2}{(\gamma + 1)M_1^2 \sin^2\beta} \quad (1)$$

For given upstream Mach number  $M_1$ , this is an implicit relation between  $\theta$  and  $\beta$ . With some trigonometric substitutions and rearrangement, Eq. (1) can be cast explicitly for  $\theta$  as

$$\tan\theta = \frac{2 \cot\beta(M_1^2 \sin^2\beta - 1)}{M_1^2(\gamma + \cos 2\beta) + 2} \quad (2)$$

which gives  $\theta$  as an explicit function of  $M_1$  and  $\beta$ .

In many problems with weak shocks determined by the deflection direction of flow (as shown in Fig. 1), the evaluation of the wave angle  $\beta$  in terms of the values of  $\theta$  and  $M_1$  is often required. This is commonly obtained from the charts related to Eq. (1), which can be inconvenient. Therefore, it is of significance to give an expression that formulates  $\beta$  as an explicit function of  $M_1$  and  $\theta$  for weak shock waves.

We encountered this problem in the research subject of shock wave/turbulent boundary-layer interactions and derived an approximate formula to evaluate  $\beta$  with the values of  $\theta$  and  $M_1$ .

### Derivation of Equations

When we rearrange Eq. (1), the following equation may be solved:

$$M_1^2 \sin^2\beta - 1 = \frac{\gamma + 1}{2} M_1^2 \frac{\sin\beta \sin\theta}{\cos(\beta - \theta)} \quad (3)$$

For small deflection angle  $\theta$ , Eq. (3) may be approximated by the following equation as that in Ref. 1

$$M_1^2 \sin^2\beta - 1 \approx \left( \frac{\gamma + 1}{2} M_1^2 \tan\beta \right) \theta \quad (4)$$

When  $\theta$  is small, the wave angle  $\beta$  approaches  $\pi/2$  for strong waves of Mach number  $M_2 < 1$  or goes to the Mach angle  $\mu$  for weak waves of Mach number  $M_2 > 1$ . Only the latter case is considered here. Therefore, when  $\theta = 0$ , the wave angle is equal to the Mach angle

$$\tan\beta = \tan\mu = \frac{1}{\sqrt{M_1^2 - 1}} \quad (5)$$

Using trigonometric identities,

$$\sin^2\beta = \frac{\tan^2\beta}{1 + \tan^2\beta} \quad (6)$$

Equation (4) may be then written as

$$\tan^2\beta = \frac{1}{M_1^2 - 1} + \frac{\gamma + 1}{2} \frac{M_1^2}{M_1^2 - 1} (\tan\beta + \tan^3\beta)\theta \quad (7)$$

Because of  $\theta \ll 1$  for the considered range of deflection angle  $\theta$ , we can assume a polynomial for  $\tan\beta$  in terms of the angle  $\theta$

$$\tan\beta = a + b\theta + c\theta^2 + \dots \quad (8)$$

where constants  $a$ ,  $b$ , and  $c$  are the functions of  $M_1$  only. Thus,

$$\tan^2\beta = a^2 + 2ab\theta + (2ac + b^2)\theta^2 + \dots \quad (9)$$

$$\tan^3\beta = a^3 + 3a^2b\theta + (3ab^2 + 3a^2c)\theta^2 + \dots \quad (10)$$

Substituting Eqs. (8) and (10) into Eq. (7), we have

$$\begin{aligned} \tan^2\beta = & \frac{1}{M_1^2 - 1} + \frac{\gamma + 1}{2} \frac{M_1^2}{M_1^2 - 1} [(a^3 + a) + (3a^2b + b)\theta \\ & + (3ab^2 + 3a^2c + c)\theta^2 + \dots] \theta \end{aligned} \quad (11)$$

Comparing Eqs. (9) and (11), we obtain

$$a = \frac{1}{\sqrt{M_1^2 - 1}} \quad (12a)$$

$$b = \frac{\gamma + 1}{4} \frac{M_1^4}{(M_1^2 - 1)^2} \quad (12b)$$

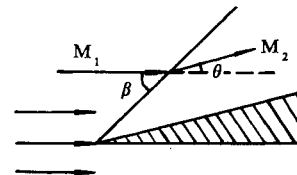


Fig. 1 Flow through an oblique shock wave.

Received Jan. 4, 1991; revision received May 20, 1991; accepted for publication May 20, 1991. Copyright © 1991 by the American Institute of Aeronautics and Astronautics, Inc. All rights reserved.

\*Lecturer and Candidate for Ph.D., Fluid Mechanics Institute.

†Professor, Fluid Mechanics Institute.